

Supporting Information

Promoting gene transfection by ROS responsive silicon nanowire arrays

Benben Lu, Hengxiao Wang, Xiang Shen, Kunyan Lu, Hongwei Wang* and Lin Yuan*

Key Lab of Health Chemistry and Molecular Diagnosis of Suzhou, Department of Polymer Science and Engineering, College of Chemistry, Chemical Engineering and Materials Science, Soochow University, Suzhou 215123, PR China

*Corresponding authors.

E-mail address: wanghw@suda.edu.cn (H. Wang), yuanl@suda.edu.cn (L. Yuan).

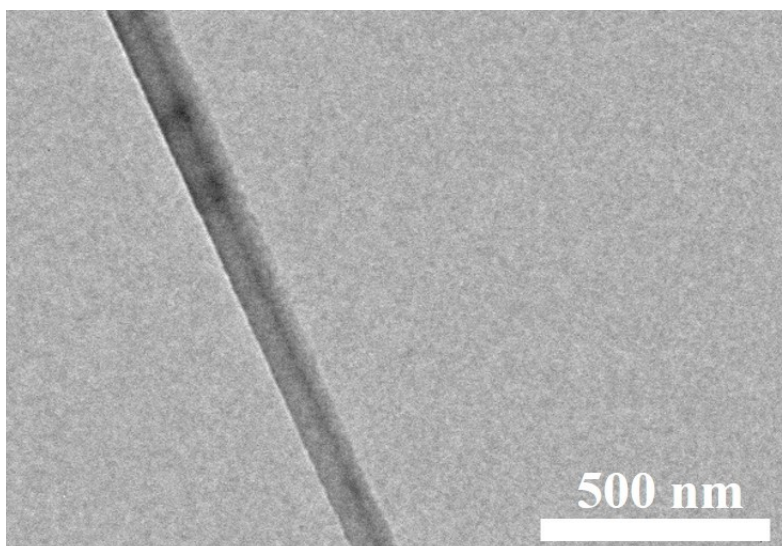


Fig. S1 TEM image of single silicon nanowire.

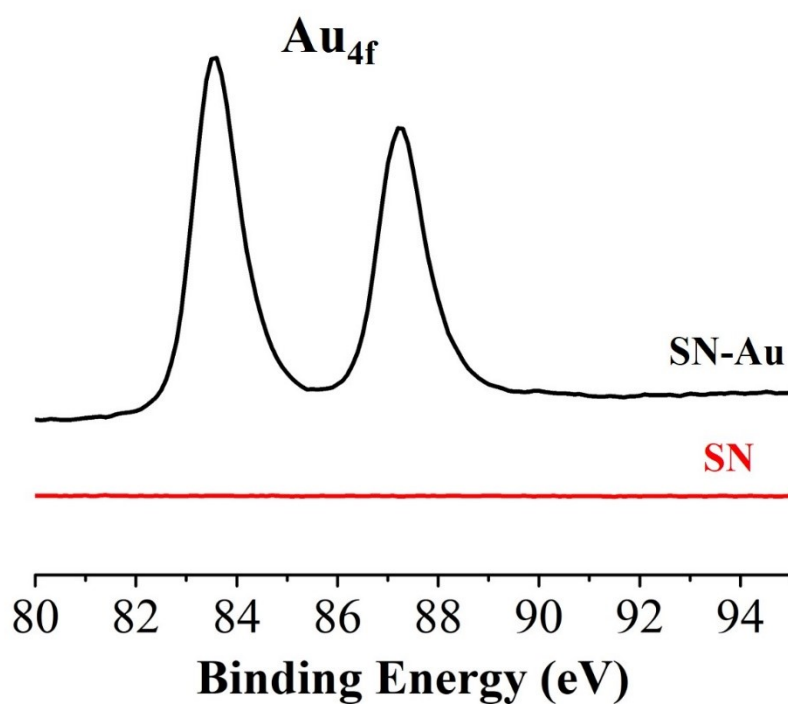


Fig. S2 High-resolution XPS spectra of the Au elements appearing on the surface of SN-Au.

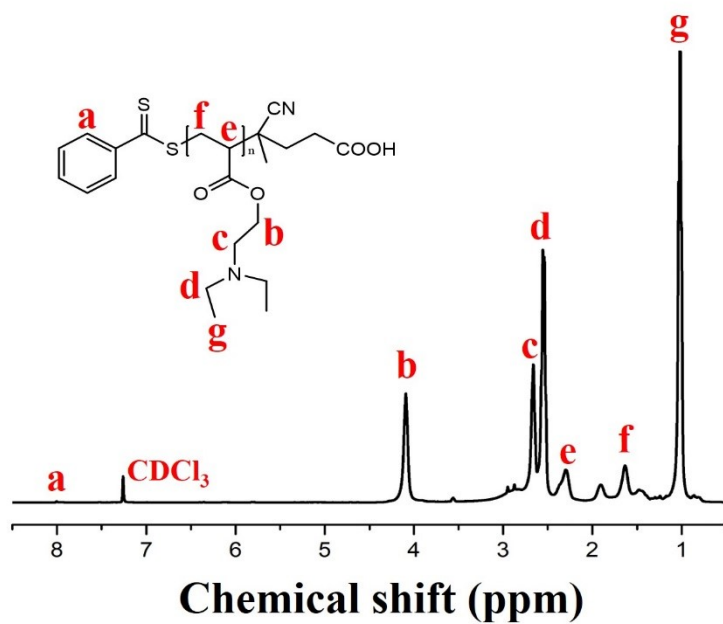


Fig. S3 ¹H-NMR spectrum of PDEAEA.

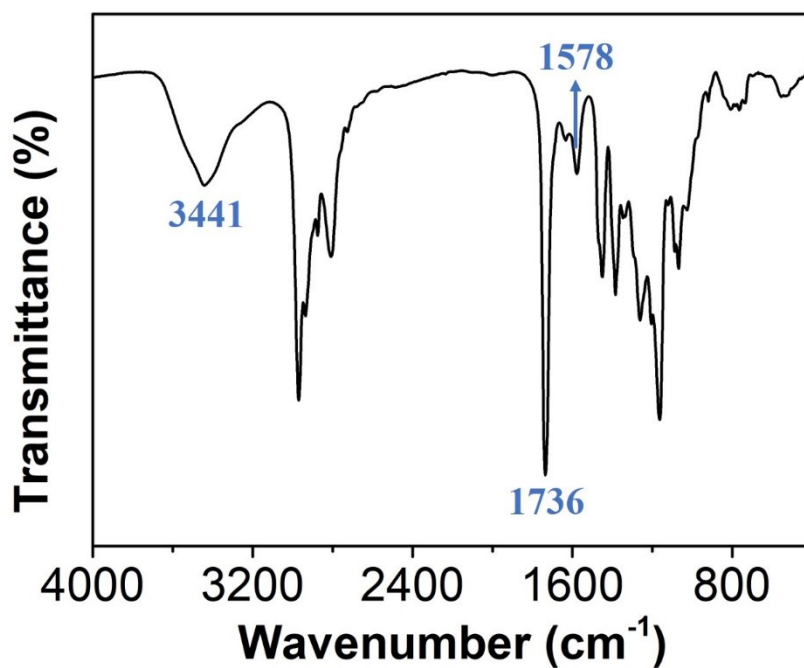


Fig. S4 FT-IR spectrum of PDEAEA.

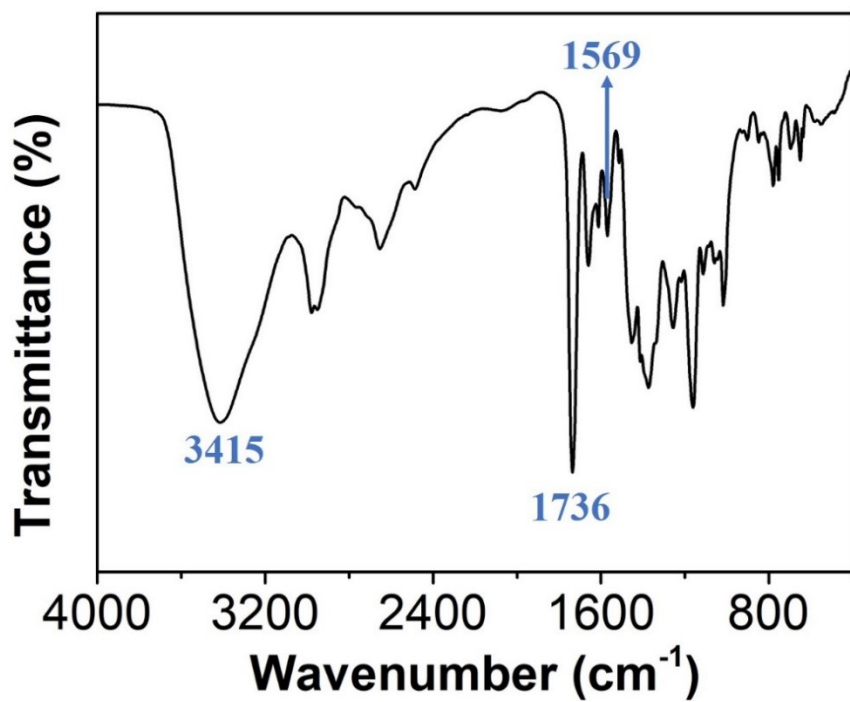


Fig. S5 FT-IR spectrum of B-PDEAEA.

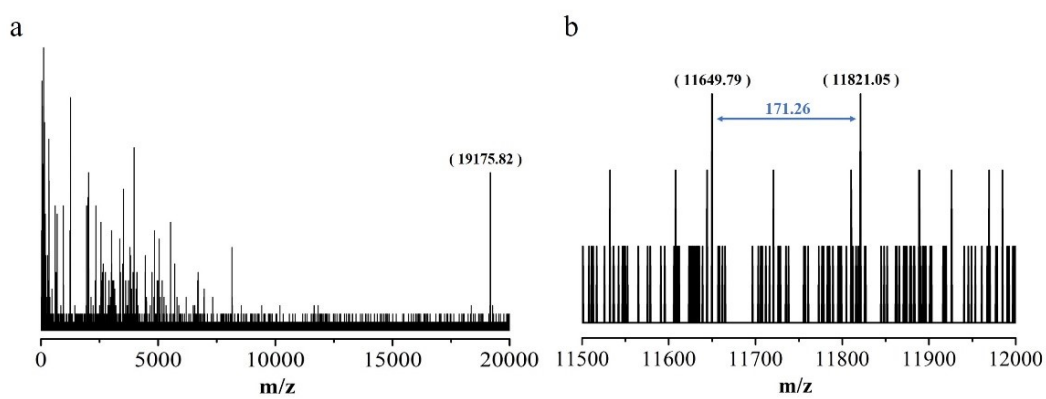


Fig. S6 (a) Mass spectra of PDEAEA and (b) partial mass spectra.

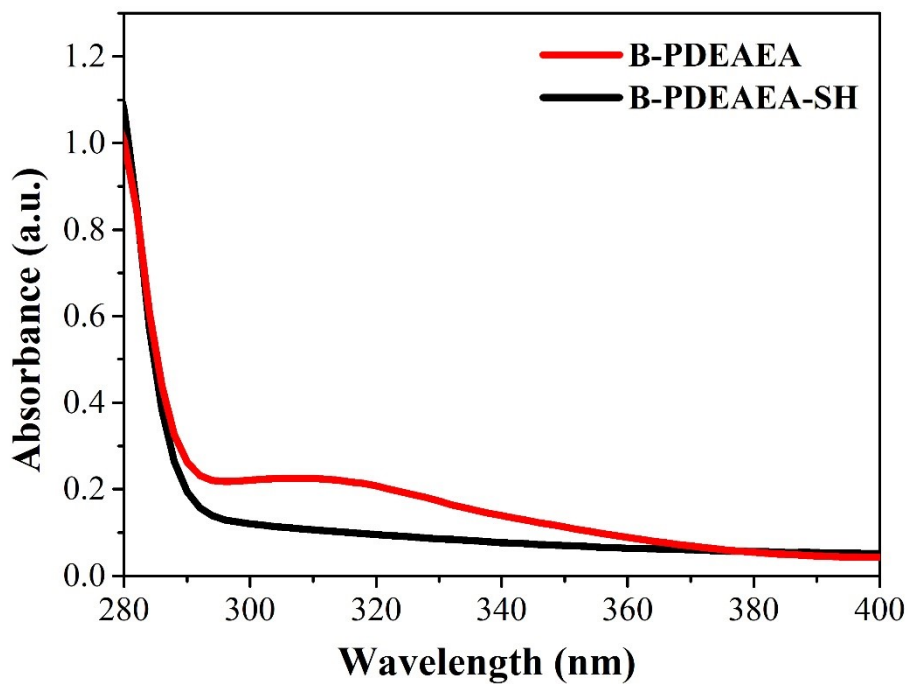


Fig. S7 UV-Vis absorbance of B-PDEAEA/ B-PDEAEA-SH.

Table S1. Elemental composition from XPS of SN surfaces at different stages of modification.

	Elemental composition (%)				
	Si	Au	C	N	O
SN	39.5	N. D.	19.7	0.8	40.0
H-SN	64.2	N. D.	24.4	N. D.	11.4
SN-Au-P	16.4	2.6	46.6	6.3	28.1

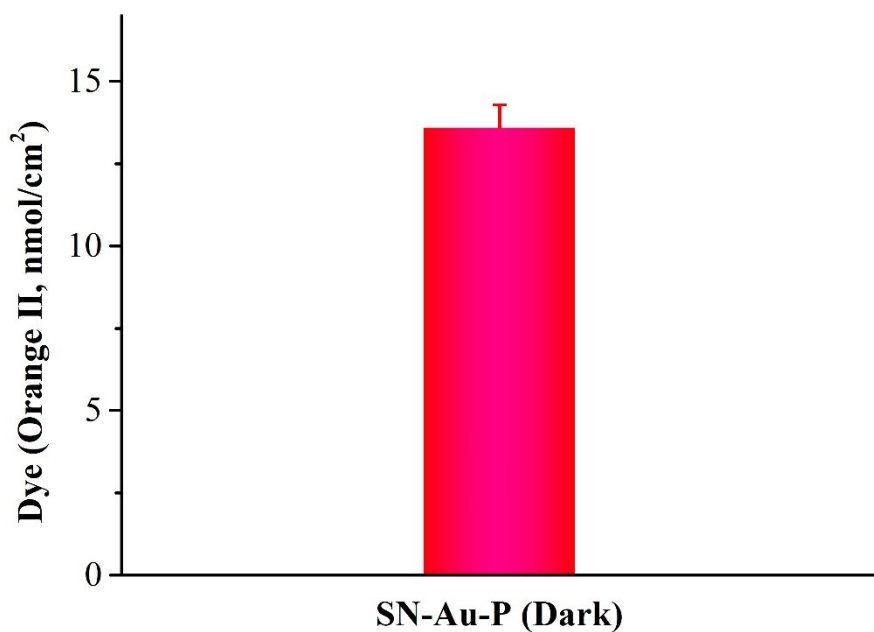


Fig. S8 The amount of Orange II dye bound to SN-Au-P surface.

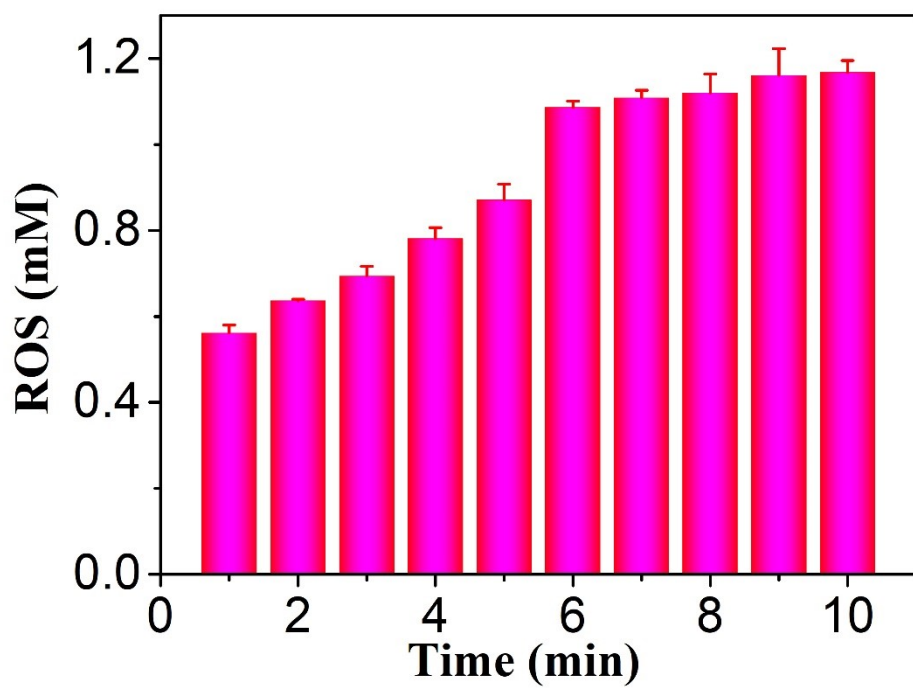


Fig. S9 The photocatalytic properties of SN-Au.

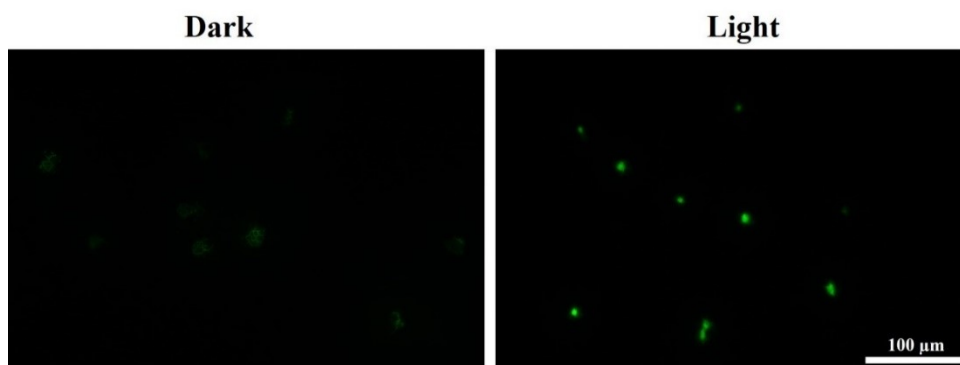


Fig. S10 DCF of HeLa cells on SN-Au-P under dark or light treatment.

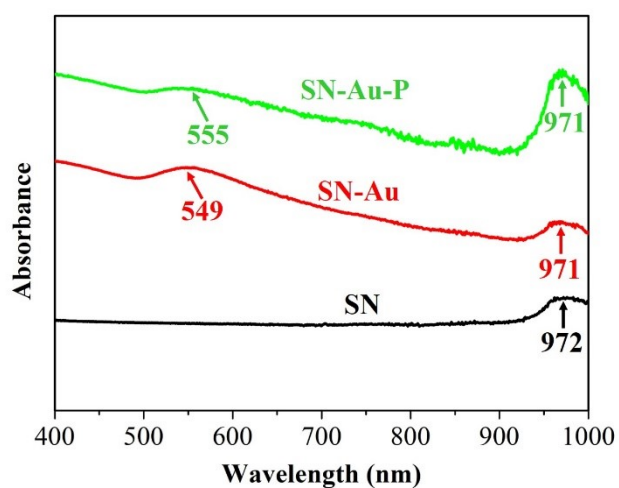


Fig. S11 Absorption spectra of SN, SN-Au and SN-Au-P.

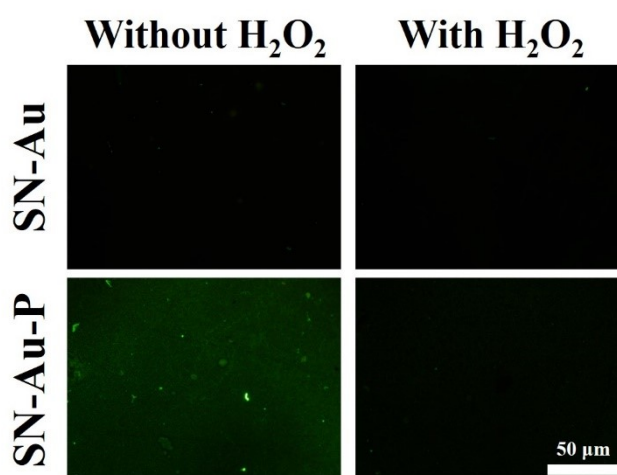


Fig. S12 Fluorescence images of different surfaces with adsorbed FITC-OVA before and after H_2O_2 treatment.

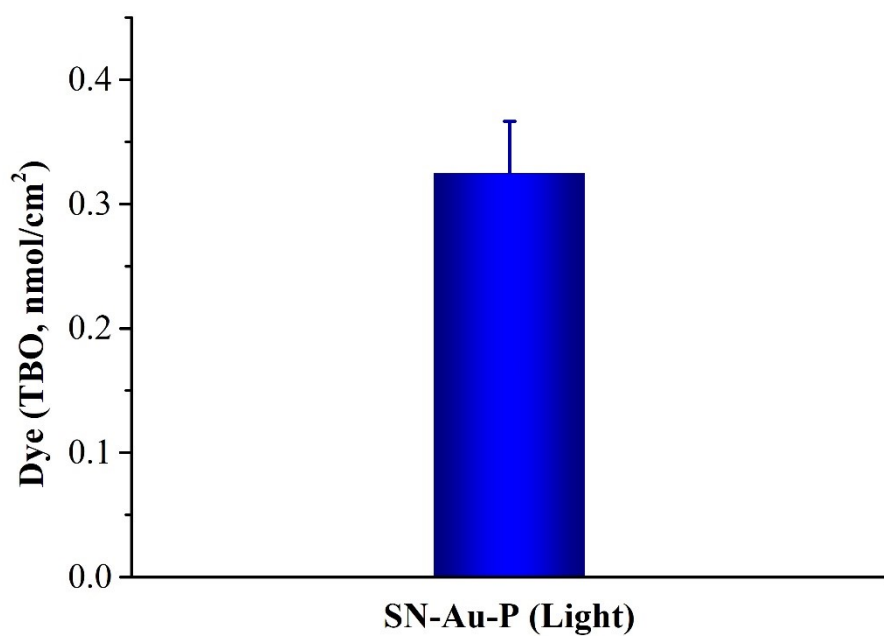


Fig. S13 The amount of TBO dye bound to SN-Au-P surface after light treatment.

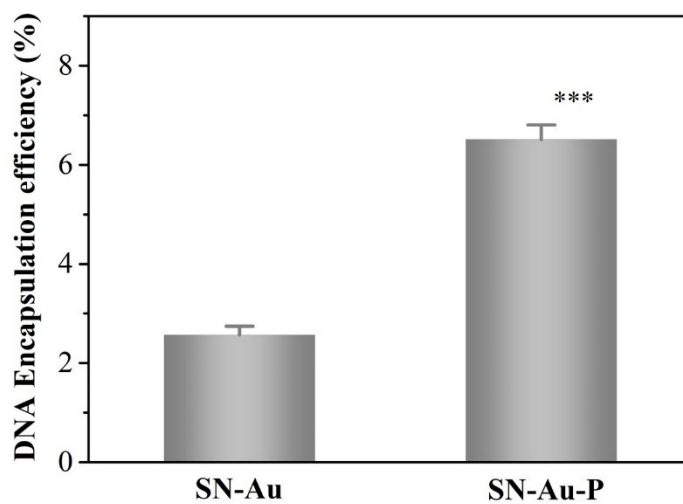


Fig. S14 DNA loading efficiency of SN-Au and SN-Au-P. Data shown as mean \pm SD, n = 3 (***) $p < 0.001$, SN-Au was the control group for analysis of significant differences).

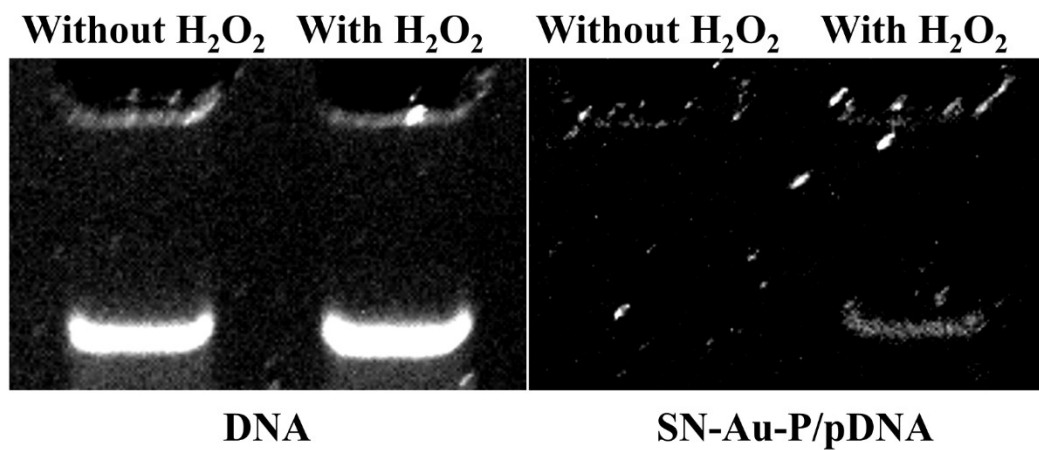


Fig. S15 Agarose gel electrophoresis assay of DNA released from the surface of SN-Au-P before and after H₂O₂ treatment.

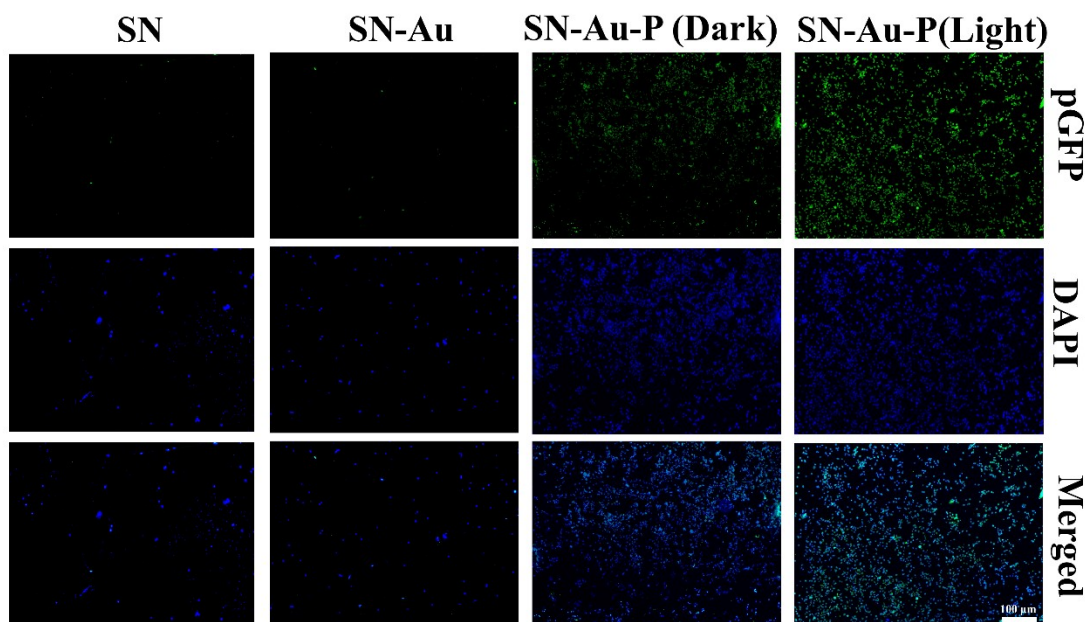


Fig. S16 Low-magnification fluorescence images of HeLa cells.

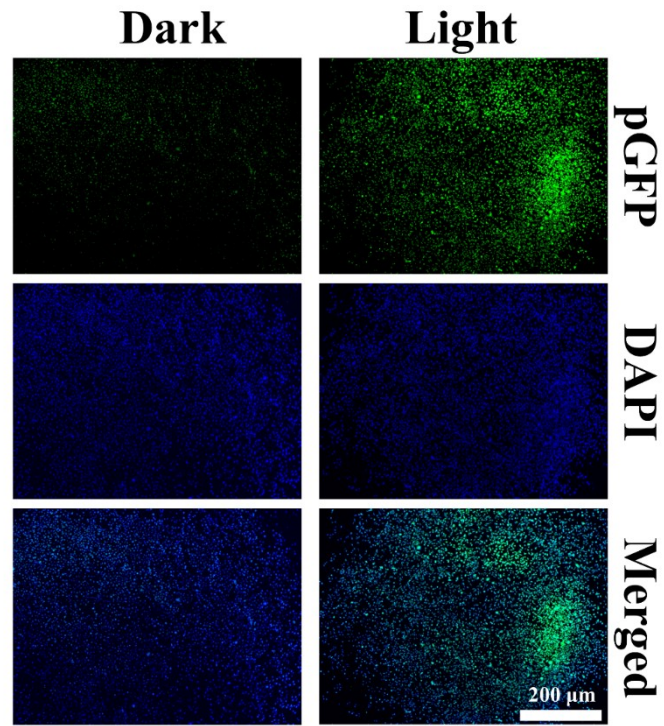


Fig. S17 Low-magnification fluorescence images of L929 cells.

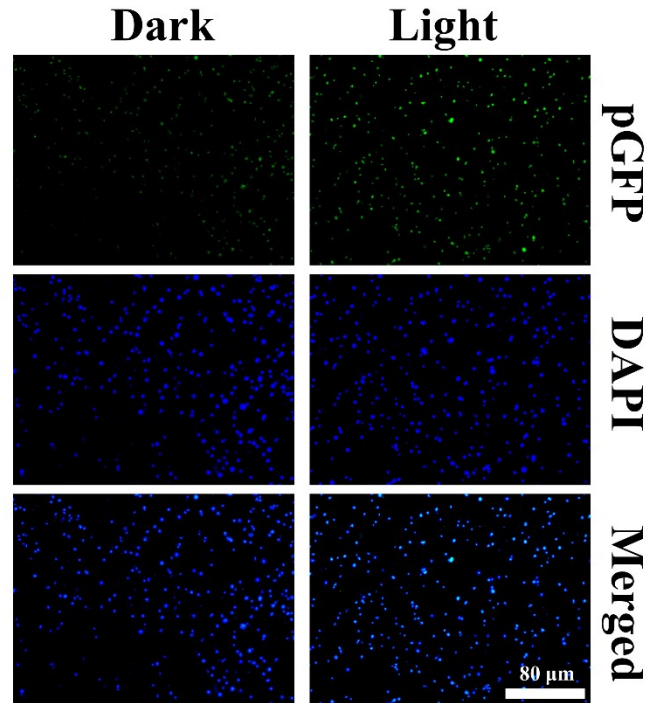


Fig. S18 Low-magnification fluorescence images of BMSC cells.

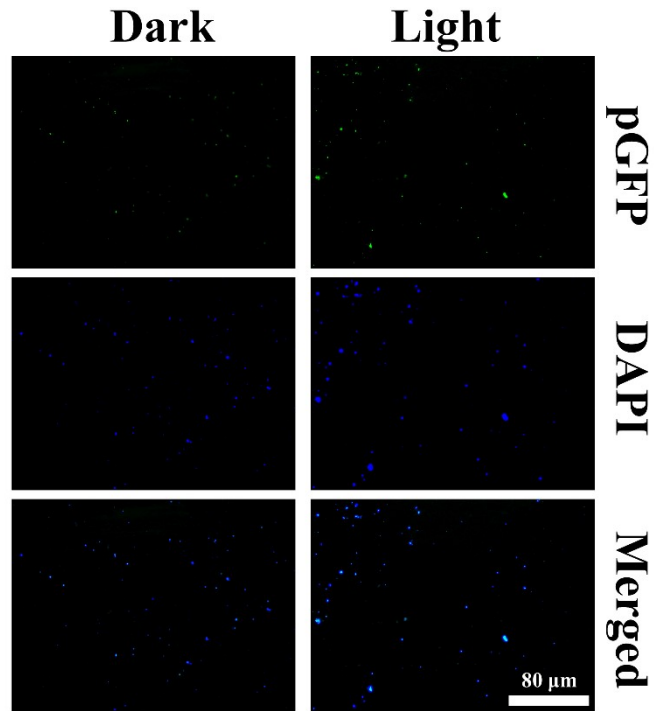


Fig. S19 Low-magnification fluorescence images of mESC cells.

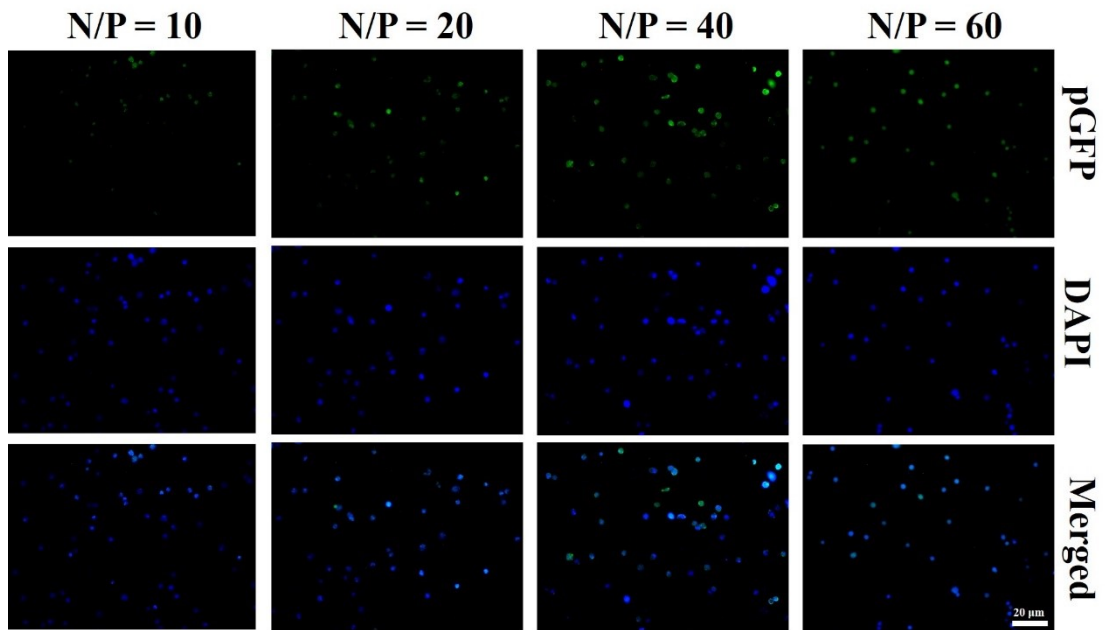


Fig. S20 Fluorescence images of HeLa cells under various N/P ratios.

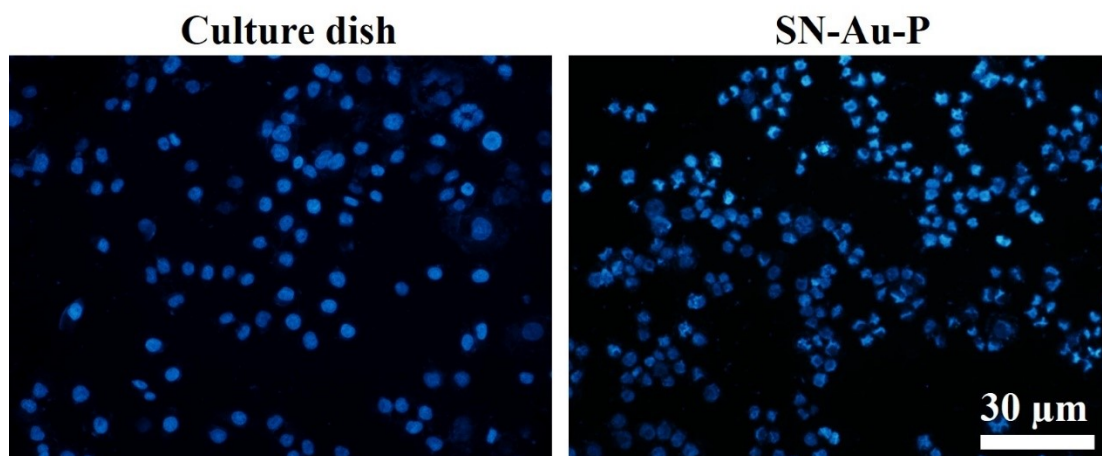


Fig. S21 Cell nucleus on the culture dish and SN-Au-P (the nucleus was stained by DAPI dye).

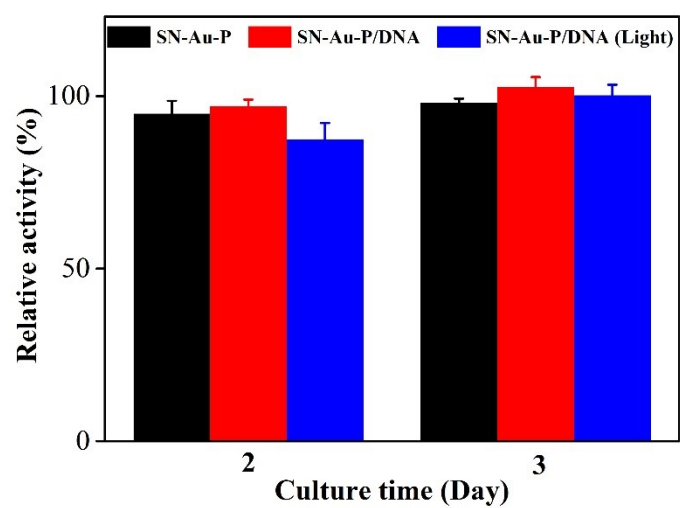


Fig. S22 CCK-8 assay of HeLa cells on different surfaces. The same density of HeLa cells on the surface of SN-Au was used as control. Data shown as mean \pm SD, n = 3.

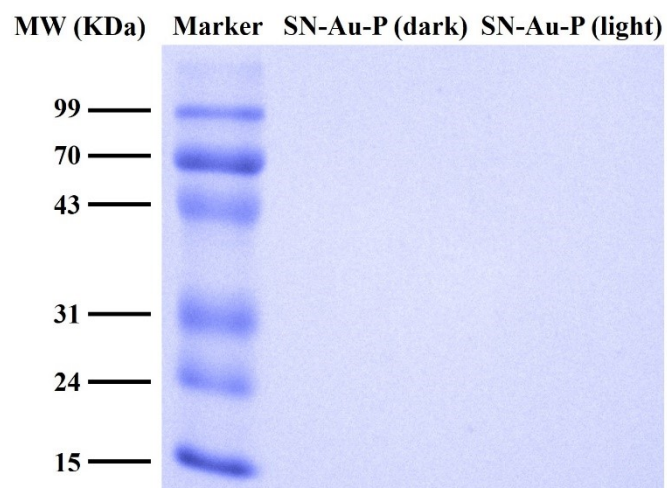


Fig. S23 SDS-PAGE of proteins in the suspension of HeLa cells on SN-Au-P under dark or light treatment.

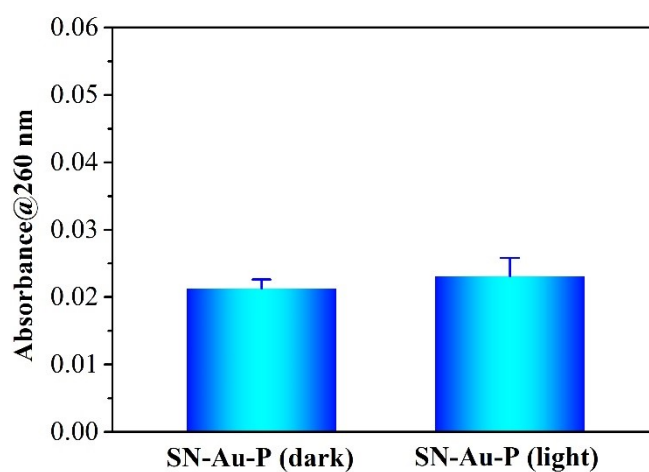


Fig. S24 The ultraviolet absorbance (260 nm) in the suspension of HeLa cells on SN-Au-P under dark or light treatment. Data shown as mean \pm SD, n = 3.